

## Synthesis of Fe–Si–B–Mn-based nanocrystalline magnetic alloys with large coercivity by high energy ball milling

P D REDDI<sup>1</sup>, N K MUKHOPADHYAY<sup>1</sup>, B MAJUMDAR<sup>2</sup>, A K SINGH<sup>2</sup>, S S MEENA<sup>3</sup>, S M YUSUF<sup>3</sup> and N K PRASAD<sup>1,\*</sup>

<sup>1</sup>Department of Metallurgical Engineering, Indian Institute of Technology, Banaras Hindu University, Varanasi 221 005, India

<sup>2</sup>Defence Metallurgical Research Laboratory, Kanchanbagh, Hyderabad 500 058, India

<sup>3</sup>Solid State Physics Division, Bhabha Atomic Research Centre, Mumbai 400 085, India

MS received 24 June 2013; revised 15 July 2013

**Abstract.** Alloys of Fe–Si–B with varying compositions of Mn were prepared using high energy planetary ball mill for maximum duration of 120 h. X-ray diffraction (XRD) analysis suggests that Si gets mostly dissolved into Fe after 80 h of milling for all compositions. The residual Si was found to form an intermetallic Fe<sub>3</sub>Si. The dissolution was further confirmed from the field emission scanning electron microscopy/energy dispersive X-ray analysis (FE-SEM/EDX). With increased milling time, the lattice parameter and lattice strain are found to increase. However, the crystallite size decreases from micrometer (75–95 μm) to nanometer (10–20 nm). Mössbauer spectra analysis suggests the presence of essentially ferromagnetic phases with small percentage of super paramagnetic phase in the system. The saturation magnetization ( $M_s$ ), remanance ( $M_r$ ) and coercivity ( $H_c$ ) values for Fe–0Mn sample after 120 h of milling were 96.4 Am<sup>2</sup>/kg, 11.5 Am<sup>2</sup>/kg and 12.42 k Am<sup>-1</sup>, respectively. However, for Fe–10Mn–5Cu sample the  $M_s$ ,  $H_c$  and  $M_r$  values were found to be 101.9 Am<sup>2</sup>/kg, 10.98 kA/m and 12.4 Am<sup>2</sup>/kg, respectively. The higher value of magnetization could be attributed to the favourable coupling between Mn and Cu.

**Keywords.** Mechanical alloying; lattice strain; amorphization; magnetic properties.

### 1. Introduction

Various non-equilibrium processing techniques have been employed during the past few decades to develop novel and advanced materials with improved performance. Amongst such processes, mechanical milling/alloying has received considerable attention from researchers (Koch 1993; Suryanarayana *et al* 2001). Mechanical milling/alloying is employed for the synthesis of amorphous and other materials including rare earth permanent magnets and ferrites (Okumura *et al* 1992; Koch 1993; Suryanarayana *et al* 2001). During this process, long-range order of the materials is disrupted to produce an intermetallic or alloy or an amorphous phase of nanometric dimension (Koch 1993; Suryanarayana *et al* 2001). The milling process depends on the factors like type of mill, balls and container, milling speed, milling time, size of starting powder, grinding medium, ball-to-powder weight ratio, extent of rolling the vial, milling atmosphere and temperature of milling (Okumura *et al* 1992; Koch 1993). Components produced after the compaction and sintering of milled powder find structural

applications in aerospace and chemical industries. Production of magnetic components by this method opens up new possibilities.

Magnetic soft alloys based on Fe are key to success of power electrical industry, where these alloys are used in transformers, chokes, filters, etc whereas hard magnetic materials are used as permanent magnets. These soft magnetic materials have high saturation magnetization and suitable values of coercivity, remanance and resistivity for such applications (Filho *et al* 2000; Yapp *et al* 2000). In contrast, it is extremely difficult to process the high silicon content (>4 wt%) Fe–Si alloys by conventional methods due to the limited solubility of Si. Nevertheless, there are a number of reports on the production of Fe–Si based alloy with other elements like B, Mn, Al, etc by high energy ball milling (Perez *et al* 1995; Liu *et al* 1999; Yapp *et al* 2000; Hosseini and Bahrami 2005). The magnetic and Mössbauer studies on such materials are a few.

Here, we report the synthesis of Fe–Si–B system with increased weight percentage of Mn using high energy ball mill. The effect of Mn on the structural and magnetic behaviour of Fe–Si–B was studied using X-ray diffraction (XRD), scanning electron microscope (SEM), vibrating sample magnetometer (VSM) and Mössbauer spectroscopy.

\*Author for correspondence (nandkp.met@itbhu.ac.in)

**Table 1.** Compositions and designations of various samples used in present study. Magnetic parameters such as  $M_s$  (Am<sup>2</sup>/kg),  $M_r$  (Am<sup>2</sup>/kg) and  $H_c$  (kA/m) for various samples (obtained after 120 h of milling) are also listed.

Sample	Sample name	Composition (wt%)					Magnetic parameters		
		Fe	Si	B	Mn	Cu	$M_s$	$M_r$	$H_c$
Fe-6Si-8B	Fe-0Mn	86	6	8	0	0	96.4	11.5	12.42
Fe-6Si-8B-1Mn	Fe-1Mn	85	6	8	1	0	134.8	9.4	10.27
Fe-6Si-8B-5Mn	Fe-5Mn	81	6	8	5	0	84.3	10.5	8.52
Fe-6Si-8B-10Mn	Fe-10Mn	76	6	8	10	0	64.7	7.6	8.44
Fe-6Si-8B-10Mn-5Cu	Fe-10Mn-Cu	71	6	8	10	5	101.9	12.4	10.98

It has been reported that Cu which is a diamagnetic, after alloying with Mn can provide a magnetic moment of up to 2.4  $\mu_B$  per atom (Bacon 1962). Hence, we added Cu in the system to observe its effect on the structural and magnetic behaviours.

## 2. Experimental

Powders of iron, silicon, boron, manganese and copper of purity 99.5, 98.5, 99, 99 and 99.5%, respectively and corresponding particles size of 53, 74, 74, 74 and 78  $\mu m$  were selected for the present study. All the powders were from LOBA CHEMIE and were used without any further modifications. Various samples of iron-based alloys with different compositions of Fe, Si, B, Mn and Cu were prepared using high energy P5-planetary ball mill (PM 400, Retsch®). The compositions and designations of the various samples are listed in table 1.

Elemental powders of above stated compositions were initially mixed and then ball milled up to 120 h. Milling was carried out in stainless steel vials of 250 mL and using 39 stainless steel balls, each one having a diameter of 10 mm and weight of 7.692 g. Ball to powder (BPR) ratio was maintained as 10:1 during each milling process. The rotational speed of the mill was kept around 200 rpm. Milling was carried out in wet condition using toluene, which restricts oxidation of metal or alloys during the process. The mill was stopped for 30 min after 5 h of run. Samples were collected after an interval of 40, 60, 80, 100 and 120 h of milling for structural, microstructural and magnetic characterizations.

Structural characterization of various milled samples was carried out using powder XRD (PHILIPS, X'PERT PRO) having CuK $\alpha$  radiation in the range of 20–90°. Phase identification is performed by the usual method of comparative peak matching with the standard ICDD software. The crystallite size ( $D$ ) and lattice strain ( $e$ ) for mechanically milled powders were calculated from single line broadening of XRD peaks using Voigt modelling (Yadav et al 2005).

The crystallite size of the samples could be estimated as:

$$D = (\lambda/\beta_C \cos\theta), \quad (1)$$

where  $\beta_C$  = Cauchy component width =  $(a_0 + a_1\psi + a_2\psi^2)$   
 $\beta$ ,  $\lambda$  = wavelength:

$$\theta = \text{Bragg angle}, \psi = 2\omega/\beta,$$

$\beta$  = integral breadth = total area under the peak divided by height of the peak and  $a_0 = 2.0207$ ,  $a_1 = -0.4803$ ,  $a_2 = -1.7756$  from Cauchy constants from the Langford table.

The lattice strain could be calculated as (Yadav et al 2005):

$$e = (\beta_G/4\tan\theta), \quad (2)$$

where  $\beta_G$  = Gaussian component =  $(b_0 + b_{1/2}(\psi - 2/\pi)^{1/2} + b_1\psi + b_2\psi^2)\beta$  and  $b_0 = 0.6420$ ,  $b_{1/2} = 1.4187$ ,  $b_1 = -2.2043$ ,  $b_2 = 1.8706$  are the Gaussian constants.

The morphology of the ball milled powder was observed by SEM (FESEM, QUANTA 200 F). Energy dispersive X-ray analysis (EDX) software associated with SEM was used for quantitative analysis. Determination of the valence states as well as magnetic nature of Fe for the as powdered samples was done using Mössbauer spectroscopy (Nucleonix Systems Pvt. Ltd.). The detail about the process has been explained earlier (Prasad et al 2005). In brief, the spectrometer was operated in constant acceleration mode (triangular wave) in transmission geometry. Rh matrix with Co<sup>57</sup> of strength 50 mCi was used as a source. The velocity scale was calibrated using an  $\alpha$ -Fe metal foil (speed 0.29 mm/s). All the spectra were fitted using WinNormos fit programme assuming Lorentzian line shapes. In addition, magnetic characterization for saturation magnetization ( $M_s$ ), remanent magnetization ( $M_r$ ) and coercive field strength ( $H_c$ ) values for as-prepared samples were carried out at 300 K using a VSM (Lakeshore, model 7410).

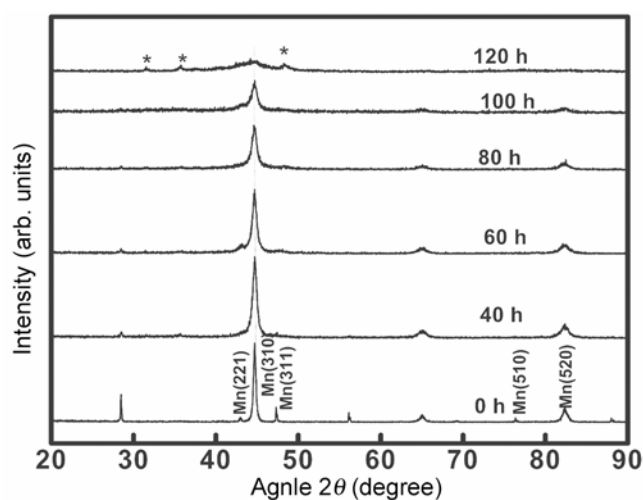
## 3. Results and discussion

Figure 1 shows XRD patterns for Fe-0Mn samples obtained after milling for different durations (40, 60, 80, 100 and 120 h). The patterns suggest that the samples obtained after 60 h of milling do not show any peak of silicon. However, after 80 h of milling, the evolution of new phase (Fe<sub>3</sub>Si) is observed. The formation of the

phase becomes prominent with increased milling time such as 100 and 120 h. This suggests that B or Si were not completely dissolved after 60 h of milling. Some parts of these elements might be soluble in iron and the rest might be contributing to the formation of new phase. The earlier study in this system also suggests that although the peaks of Si or B were not observed in XRD patterns, but they were found as a separate phase in the SEM analysis even after 64 h of milling (Perez *et al* 1995). It was observed that with increased milling time, the peaks become broader, which could either be due to decrease in crystallite size or due to amorphization of the alloy. Simultaneously, the (1 1 0) peak of Fe is found to be shifting slightly towards right (i.e. higher Bragg angle) which indicate more dissolution of the alloying elements with increased milling time. Boron was added to enhance amorphization process. However, its peaks were not observed due to its low atomic scattering factor.

XRD patterns of Fe–5Mn and Fe–10Mn–5Cu powders obtained after similar milling times of 40, 60, 80, 100 and 120 h were close to that of Fe–0Mn and are shown in figures 2 and 3, respectively. For these two cases also, the disappearance of Si peaks was observed after 60 h of milling. It was found that dissolution of Si has increased with Mn content for both the samples. Similar to Fe–0Mn, these samples also showed the formation of Fe<sub>3</sub>Si phase after 80 h of milling, however, the phase was less prominent in Fe–5Mn sample and it was least in Fe–10Mn–5Cu sample. This indicates that the presence of Mn improves the dissolution of Si and B which further improves with Cu-addition. Copper was also found to contribute to amorphization and thus, the peaks for Fe–10Mn–5Cu samples become broader compared to that of Fe–0Mn and Fe–5Mn samples. There were no individual peaks for Mn or Cu or their alloys. The

samples were identified to be *bcc* structure. In contrast, researchers have observed transformation of *bcc* to *fcc* structure for Fe–24Mn and Fe–24Mn–6Si samples (Liu *et al* 1999). Similarly, other researchers have also observed the transformation of  $\alpha$ -Fe into  $\gamma$ -Fe in ball milled Fe-rich Fe–Cu powder even at a composition of Fe–34 at% Cu (Wu *et al* 1993; Majumdar *et al* 1997). However, in the present case, such transformations were not observed. This could be attributed to the presence of Si which did not allow this phase transformation. Nevertheless, the relatively less amount of substituent could be the other possibility. In contrast, the sample milled for longer duration showed amorphization due to the presence of B. The different milling conditions might also have contributed here.



**Figure 2.** X-ray diffraction patterns of Fe–5Mn powder obtained after milling for various times (\* = Fe<sub>3</sub>Si phase).

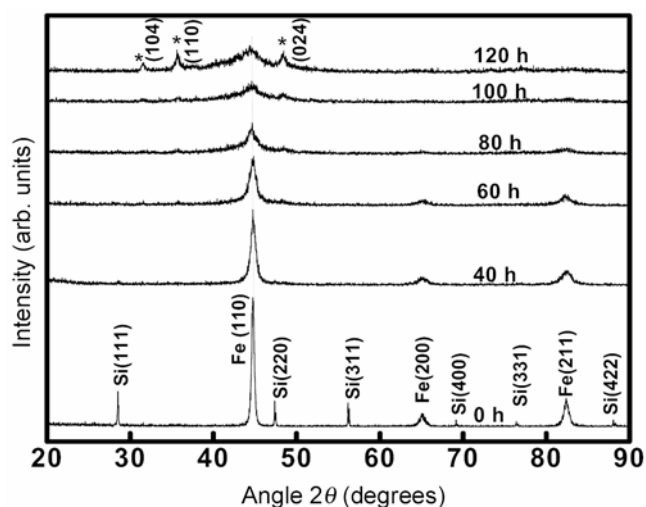


**Figure 1.** X-ray diffraction patterns of Fe–0Mn powder obtained after milling for various times (\* = Fe<sub>3</sub>Si phase).

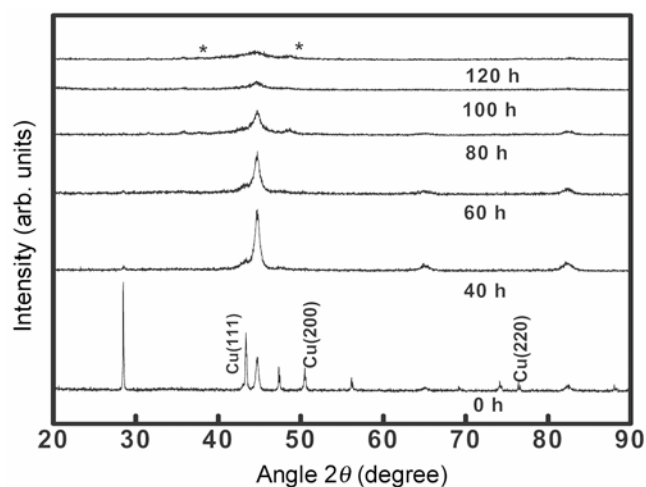


**Figure 3.** X-ray diffraction patterns of Fe–10Mn–5Cu powder obtained after milling for various times (\* = Fe<sub>3</sub>Si phase).

With increased milling time, slight shift of the peaks of XRD patterns towards the lower  $\theta$  value was observed for all three samples (figures 1–3). There was a gradual increase of lattice parameter of *bcc* Fe due to the dissolution of substituents. XRD patterns for the samples obtained after 40 h of milling had prominently one peak (figures 1–3) and thus, the lattice parameter was calculated using Voigt modelling given in (1) (Yadav *et al* 2005). The variation of lattice parameter with milling time for different samples is shown in figure 4. The reason for the increase of lattice parameter could be due to the formation of solid solution (Moumeni *et al* 2005). It was observed that the rise in the lattice parameter for the samples was not following a continuous trend. This may be because of dissimilar contribution of various elements such as Mn, Fe, Cu, Si and B having atomic radii of 1.61, 1.56, 1.45, 1.11 and 0.87 Å, respectively.

For various milled samples, the amount of lattice strain induced was also calculated using Voigt model from (2) (Yadav *et al* 2005) and the values are shown in figure 5. Due to the involvement of steady high energy forming process such as ball milling, the generations of dislocation densities in the systems are inevitable (Suryanarayana 2001; Mohamed 2003). For all the samples, the strain increased continuously with milling time. The crystallite size, estimated for various samples after different milling times using Voigt model from (1) (Yadav *et al* 2005) are shown in figure 6. Initially, crystallite size of the powders was in the range of  $\mu\text{m}$  which reduced to  $\sim 75$ – $95$  nm after 40 h of milling (figure 6). With increasing milling time, the size further reduced and it was found to be  $\sim 15$ – $25$  nm after 120 h of milling. The reduction of crystallite size of various samples can be attributed to the strain hardening and subsequent strain relaxation due to dynamic recovery caused during milling (Ares and Cuevas 2005; Ebrahimi *et al* 2011).

Typical SEM micrographs of Fe–0Mn and Fe–1Mn powders obtained after 100 h of milling are shown in figure 7. The micrographs suggest that the particles were in agglomerated form. This could be attributed to the continuous welding and fracture mechanisms during milling of ductile–ductile systems (Moumeni *et al* 2005; Ebrahimi *et al* 2011). The elemental analysis using EDX for the particles (whether grey or bright) suggests that the samples had essentially Fe and Si. There was no separate peak for Si or Fe or Mn. This further confirms the dissolution of Si in Fe which occurs during ball milling as observed in XRD results.

Mössbauer spectra analysis for the powder samples (e.g. Fe–0Mn, Fe–1Mn, Fe–3Mn, Fe–5Mn, Fe–10Mn and

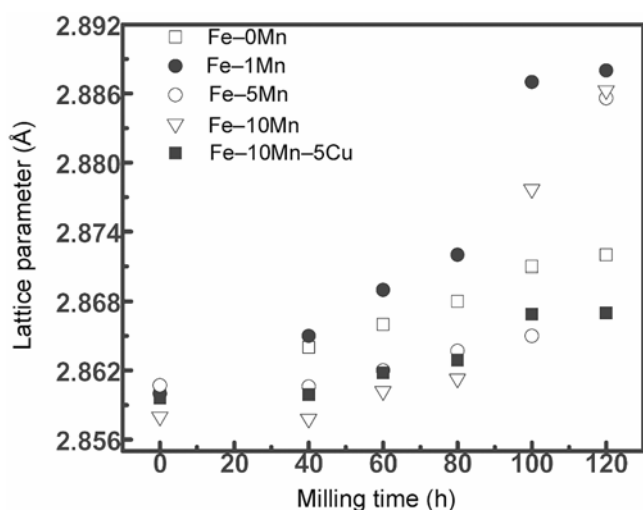


**Figure 4.** Variation of lattice parameter vs milling time for various samples.

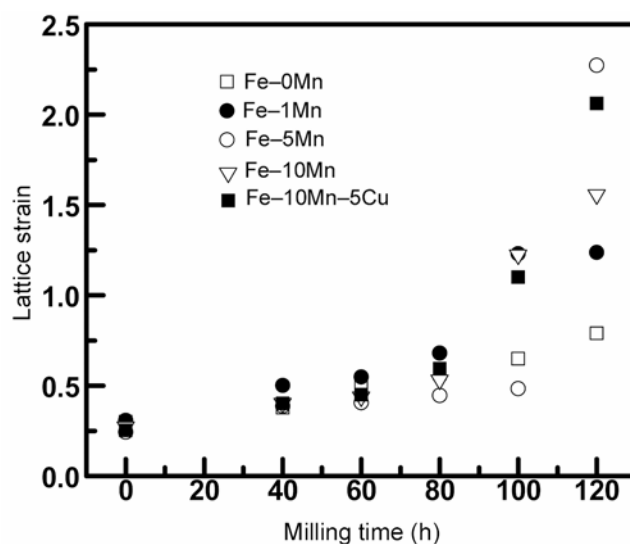


**Figure 5.** Variation of lattice strain vs milling time for various samples.

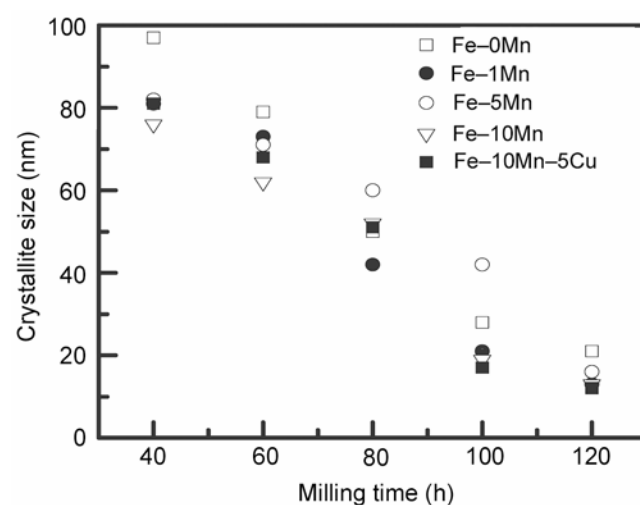


**Figure 6.** Variation of crystallite size vs milling time for various samples.

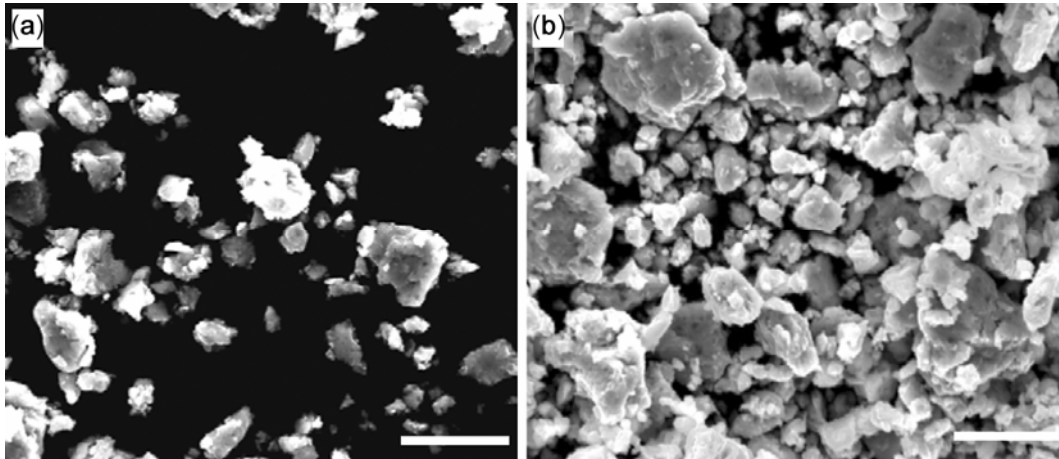


**Figure 7.** SEM micrographs of as-prepared powders after milling for 100 h: (a) Fe–0Mn and (b) Fe–1Mn. Bar = 5  $\mu\text{m}$ .

**Table 2.** Hyperfine parameter such as  $B_{\text{HF}}$  (kOe), IS (mm/s), QS (mm/s) and RA (%) for various samples (obtained after 80 h of milling).

Sample	First sextet				Second sextet				Doublet			
	$B_{\text{HF}}$	IS	QS	RA	$B_{\text{HF}}$	IS	QS	RA	$B_{\text{HF}}$	IS	QS	RA
Fe–0Mn	331	0.012	0.00	18	241	0.16	–0.01	80	–	0.34	0.81	2
Fe–1Mn	331	0.011	0.00	21	246	0.16	–0.02	77	–	0.31	0.80	2
Fe–5Mn	331	0.008	0.00	18	208	0.17	–0.01	76	–	0.42	1.25	5
Fe–10Mn	331	0.006	0.00	14	209	0.15	–0.01	81	–	0.19	1.05	5
Fe–10Mn–Cu	331	0.005	0.00	32	202	0.22	–0.07	66	–	0.35	1.08	2

Fe–10Mn–5Cu) obtained after milling for 80 h are shown in figure 8. For all the samples, the spectra show mainly two sextets and doublet. Both the sextets could be identified as iron-based phases having ferromagnetic characteristics, whereas the doublet could be due to the superparamagnetic component (Brand *et al* 1983) (figure 8). The hyperfine field ( $B_{\text{H}}$ ), quadrupole split (QS) and isomer shift (IS) values of both sextets for all samples are tabulated in table 2. The  $B_{\text{H}}$  and QS values for all the first sextets were almost constant and around 331 and 0 kOe, respectively whereas IS value is found to decrease with Mn and Cu contents. Comparing with the hyperfine field of pure iron which is 330 kOe, it can be inferred that the Fe phase is devoid of any impurity (Varret *et al* 1982). The  $B_{\text{H}}$  value for the second sextet (second Fe-based phase) for Fe–0Mn was 241 kOe which initially increases slightly for Fe–1Mn alloy and then decreases with further addition of Mn (table 2). The reduction of hyperfine field from 330 to 241 kOe indicates that the environment of Fe atoms is enriched with the other alloying elements such as Si and B, which is in conformity with the XRD results of solid solution formation. It is interesting to note that the hyperfine field increases slightly with the addition of Mn up to 1%. The dilute solution of Mn in Fe environment might lead to coupling

the spins between Fe and Mn ferromagnetically (Mirzoev *et al* 2009). Further increase of Mn favours antiferromagnetic coupling and thus decreases hyperfine field. The spectrum of Fe–10Mn–5Cu was different from the other spectra as it had relatively higher proportion of pure Fe-phase (figure 8 and table 2). This may be because of ferromagnetic coupling of Mn–Cu (Bacon 1962). For all the samples, the proportion of doublet was quite low (~2–5%), which could be due to the absence of any paramagnetic or superparamagnetic component.

The magnetization vs field curve for the samples obtained after 120 h of milling are shown in figure 9. The corresponding values of  $M_{\text{s}}$ ,  $H_{\text{c}}$  and  $M_{\text{r}}$  for various samples are listed in table 1. The  $M_{\text{s}}$  value for Fe–0Mn was found to be around 96.4 Am<sup>2</sup>/kg, which was reasonably lower than that of bulk Fe–4wt% Si (~185 Am<sup>2</sup>/kg) (Cullity 1972). The lower value of  $M_{\text{s}}$  could be due to the dissolution of alloying elements and due to the decrease in the crystallite size. The magnetic properties of the materials depend on the short-range ordering which may be described by the number, type, distance and symmetry of the nearest neighbours (Staunton *et al* 1998). The effect of dead or inert layer on the nanoparticles could also be responsible for this reduced value of  $M_{\text{s}}$ . Lower value may also be due to the surface/interface pinning forces

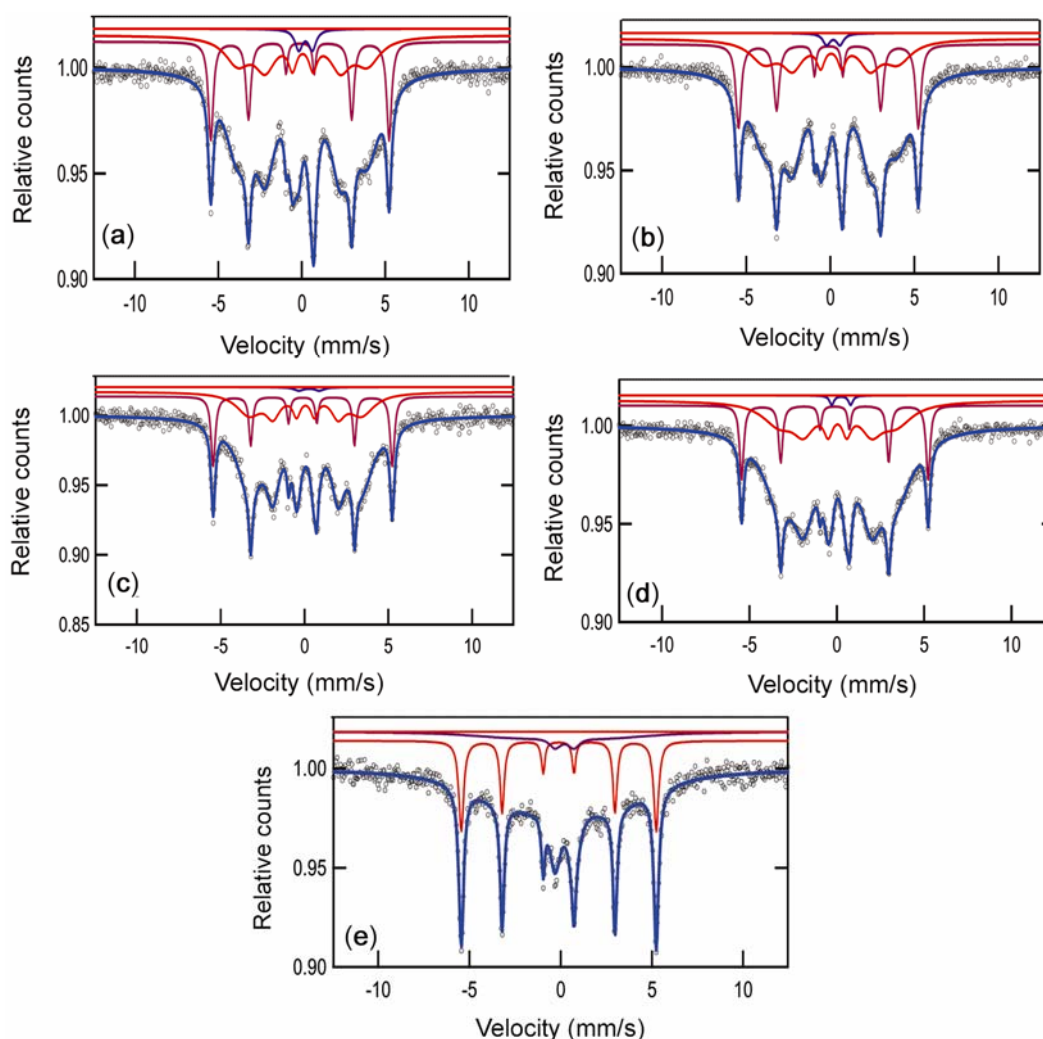


**Figure 8.** Mössbauer spectra of as-prepared powders after milling for 80 h (a) Fe-0Mn, (b) Fe-1Mn, (c) Fe-5Mn, (d) Fe-10Mn and (e) Fe-10Mn-5Cu.

which restricts the rotation of magnetization along the direction of the external field (Behvandi *et al* 2010).

Similar to the Mössbauer spectra, the  $M_s$  value initially increased and then decreased with Mn. In general, the addition of Mn in Fe reduces both  $M_s$  and  $B_H$  values due to the antiferromagnetic coupling between them (Piramanayagam *et al* 1990). Mn has high single atom magnetic moment ( $\sim 5 \mu_B$ ) as compared to that of Fe atom ( $\sim 2.6 \mu_B$ ), but couples antiferromagnetically between two Mn atoms. Therefore, when Mn is in dilute solution in Fe, the Mn-Mn interaction decreases which attributes to the escape from the formation of antiferromagnetic coupling leading to the enhancement of magnetic moment. With further increase of Mn,  $M_s$  value decreases due to the increase of Mn-Mn interaction. However, the magnetization further increases for Fe-10Mn-Cu sample as compared to that of Fe-10Mn sample. As stated earlier that diamagnetic Cu after coupling with Mn can provide a momentum up to  $2.4 \mu_B$  per atom and it could be one of the reasons for enhanced  $M_s$  value of Cu containing alloy

(Bacon 1962). The Mössbauer spectrum of the Fe-10Mn-5Cu sample (figure 8 and table 2) also shows similar behaviour.

The  $H_c$  value for various samples obtained after milling for 120 h are given in table 1. The coercivity for the samples was relatively higher ( $\sim 8.44$ – $12.42 \text{ kAm}^{-1}$ ). It was even higher than the value reported for ball-milled product of Fe-Co-V or Fe-Ni system (Behvandi *et al* 2010). Magnetic coercivity is an extrinsic and structure sensitive characteristic which essentially depends on the material structure, internal defects, residual stresses, grain size and nonmagnetic inclusions (Herzer 1997). It has been reported that  $H_c$  enhances due to the pinning of magnetic domain walls by the impurities or the nonmagnetic inclusions produced during mechanical alloying (Chen 1977). The large density of defects like dislocations or increased fraction of grain boundaries produced or the residual stress due to severe plastic deformation during the process also impede the domain walls movement and increase the coercivity (Bacon 1962). For Fe-10Mn-5Cu,

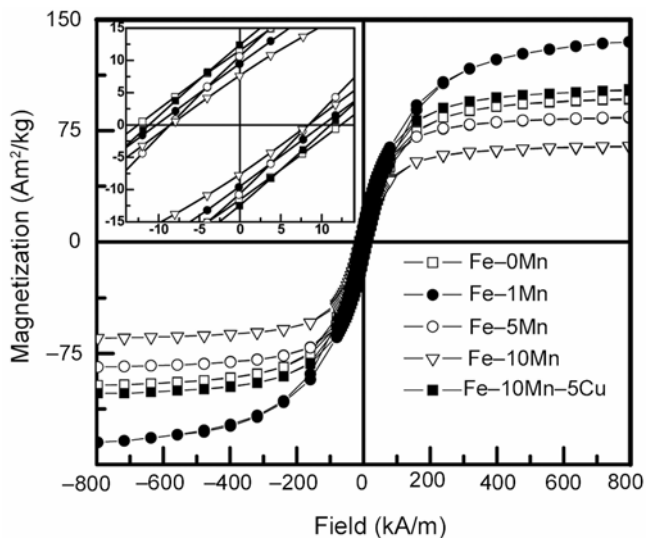


**Figure 9.** Magnetization vs applied magnetic field curve for as-prepared powders obtained after milling for 120 h.

the  $H_c$  value was 10.98 kA/m, which was higher than the values for only Mn-substituted samples. The  $M_r$  values of all the samples were also relatively higher (table 1). Nevertheless, similar to  $M_s$  and  $H_c$  values, the  $M_r$  value initially increases and then decreases with increased Mn-addition (table 2), whereas the sample with Cu constituents had highest  $M_r$  value. The higher values of  $M_s$ ,  $H_c$  and  $M_r$  for Fe–10Mn–5Cu sample could be due to the suitable coupling between Mn and Cu (Bacon 1962).

#### 4 Conclusions

Using high energy planetary ball mill, various alloys of Fe–Si–B with varying composition of Mn/Cu were prepared. Almost a complete dissolution of Si was found after 80 h of milling but it took lesser time in the case of high Mn and Cu substitution. The dissolution of alloying elements in Fe was confirmed by XRD and FESEM/EDX study directly and indirectly by magnetic characterization. Due to the formation of alloys, the lattice parameter enhanced from 2.8581 to 2.8881 Å and strain increased from 0.25 to 2.25, whereas the crystallite size decreased from micrometer to nanometer (10–20 nm). Mössbauer spectra analysis suggests the presence of essentially ferromagnetic components in the system. Although, the  $M_s$  value for the milled samples (64.7–134.8 Am<sup>2</sup>/kg) was less than the bulk counterpart, but it was relatively higher for the samples containing low Mn or both Mn and Cu. The  $M_r$  value was in the range of 7.6–12.4 Am<sup>2</sup>/kg, whereas  $H_c$  value was in the range of 8.44–12.42 kA/m, which was relatively more, hence, may provide better squareness ratio.

#### Acknowledgement

(NKP) and (NKM) thank DST, New Delhi, India, for financial support to sanction project related to magnetic materials and ball milling, respectively.

#### References

- Ares J R and Cuevas F 2005 *Acta Mater.* **53** 2157  
 Bacon G E 1962 *Proc. Phys. Soc.* **79** 938  
 Behvandi A, Shokrollahi H, Chitsazan B and Ghaffari M 2010 *J. Magn. Magn. Mater.* **322** 3932  
 Brand R A, Lauer J and Herlach D M 1983 *J. Phys. F: Met. Phys.* **13** 675  
 Chen C W 1977 *Magnetism and metallurgy of soft magnetic materials* (Amsterdam: North-Holland)  
 Cullity B D 1972 *Introduction to magnetic materials* (London: Addison Wesley)  
 Ebrahimi A, Ghaffari M and Janghorban K 2011 *J. Magn. Magn. Mater.* **323** 149  
 Filho A F, Bolfarini C, Xu Y and Kiminami C S 2000 *Scr. Mater.* **42** 213  
 Herzer G 1997 *Handbook of magnetic materials* (The Netherlands: Elsevier Science B V) **Vol. 10**  
 Hosseini H R M and Bahrami A 2005 *Mater. Sci. Eng.* **B123** 74  
 Koch C C 1993 *Nanostruct. Mater.* **2** 109  
 Liu T, Liu H Y, Zhao Z T, Ma R Z, Hu T D and Xi Y N 1999 *Mater. Sci. Eng.* **A271** 8  
 Majumdar B, Raja M M, Narayanasamy A and Chattopadhyay K 1997 *J. Alloys Compd.* **248** 192  
 Mirzoev A A, Mirzaev D A and Yalolov M M 2009 *Proceedings of the World Congress on Engineering* Vol. 1, WCE 2009, London, UK, ISBN: 978-988-17012-5-1  
 Mohamed A 2003 *Acta Mater.* **51** 4107  
 Momeni H, Alleg S and Greneche J M 2005 *J. Alloys Compd.* **386** 12  
 Okumura H, Ishihara K N, Shingu P H, Park H S and Nasu S 1992 *J. Mater. Sci.* **27** 153  
 Perez R J, Huang B, Crawford P J, Sharif A A and Lavernia E J 1995 *Mater. Sci. Eng.* **A204** 217  
 Piramanayagam S N, Shringi S N, Prasad S, Nigam A K, Chandra G, Krishnan R and Ramanan V R V 1990 *Solid State Commun.* **76** 93  
 Prasad N K, Panda D, Singh S, Mukadam M D, Yusuf S M and Bahadur D 2005 *J. Appl. Phys.* **97** 10Q903  
 Staunton J B, Razee S S A, Ling M F, Johnson D D and Pinski F J 1998 *J. Phys. D: Appl. Phys.* **31** 2355  
 Suryanarayana C 2001 *Prog. Mater. Sci.* **46** 1  
 Suryanarayana C, Ivanov E and Boldyrev V V 2001 *Mater. Sci. Eng.* **A151** 304  
 Varret F, Hanzic A and Campbell I A 1982 *Phys. Rev.* **B26** 5285  
 Wu Y K, Huang J Y, He A Q, Hu K Y and Meng X M 1993 *Acta Metall. Sinica* **B29** 546  
 Yadav T P, Mukhopadhyay N K, Tiwari R S and Srivastava O N 2005 *Mater. Sci. Eng.* **A393** 366  
 Yapp R, Watts B E and Leccabue F 2000 *J. Magn. Magn. Mater.* **215** 300